IEEE/CSC & ESAS SUPERCONDUCTIVITY NEWS FORUM (global edition), October 2013
This manuscript was published by Superconductor Science & Technology (SuST, IOP) 27, No. 4, 044019, (2014).

A comparative study of $Sr_{1-x}K_xFe_2As_2$ and $SmFeAsO_{1-x}F_x$ superconducting tapes by magneto-optical imaging

Chao Yao[1], Chunlei Wang[1], Xianping Zhang[1], Dongliang Wang[1], He Lin[1], Qianjun Zhang[1], Yanwei Ma[1], Yuji Tsuchiya[2], Yue Sun[2] and Tsuyoshi Tamegai[2]

[1]Key Laboratory of Applied Superconductivity, Institute of Electrical Engineering, Chinese Academy of Sciences, Beijing 100190, China
[2]Department of Applied Physics, The University of Tokyo, Hongo, Tokyo 113-8656, Japan

E-mail: ywma@mail.iee.ac.cn

Abstract
Using the magneto-optical imaging (MOI) technique, the intergranular critical current density J_c at various temperatures and the homogeneity of the local structure of the superconducting cores for the powder-in-tube (PIT) $Sr_{1-x}K_xFe_2As_2$ and $SmFeAsO_{1-x}F_x$ tapes are systemically investigated. These two tapes have large transport J_c over 10^4 Acm^{-2} in self-field at 20 K and 4.2 K respectively, but the J_c of the $SmFeAsO_{1-x}F_x$ tape decreases rapidly with the increasing magnetic field. The MOI characterization indicates large bulk currents circulating through the whole sample for the both $Sr_{1-x}K_xFe_2As_2$ and $SmFeAsO_{1-x}F_x$ tapes, but also reveals the inhomogeneity inside the $SmFeAsO_{1-x}F_x$ sample. The results obtained from the MO measurements can be confirmed by the magnetic hysteresis measurements M(H) and the SEM examination. The weak high-field performance of the $SmFeAsO_{1-x}F_x$ tape may be ascribed to its short-time heat treatment.

Keywords: superconductivity, tapes, wires, magneto-optical imaging, critical current density

1. Introduction

The iron-based superconductors (IBS) discovered in 2008 [1] aroused extensive research works to elucidate the superconducting mechanism of this new class of superconductors. At the same time, enormous efforts were devoted to improve their superconducting properties for practical applications. With ultrahigh upper critical fields of about 300 T for 1111 type IBS (ReFeAsO, Re = rare earth elements) and over 100 T for 122 type IBS ($AeFe_2As_2$, Ae = alkali or alkali earth elements) [2-5], superconducting wires fabricated with these two types of IBS have great potential for high-field applications. Soon after the discovery of the IBS materials, the first 1111 and 122 type IBS superconducting wires were made using the powder-in-tube (PIT) method [6, 7]. However, it was found that the transport currents of IBS wires were largely deteriorated by high-angle grain boundaries [8, 9] and defects such as cracks, pores, and impurities [10-12]. In recent years, by using the *ex situ* method instead of the *in situ* method used at the early stage, the critical current density J_c of both 1111 and 122 type IBS superconducting wires has been improved continuously [13]. To date, the J_c values of *ex situ* 122 IBS wires have rapidly increased above 10^5 Acm^{-2} at 4.2 K, 0 T or 10^4 Acm^{-2} at 4.2 K, 10 T, by employing a hot isostatic pressing (HIP) [14], a combination technique of chemical addition and rolling texture [15], and cycles of cold deformation and heat treatment [16]. On the other hand, recently J_c values over 2×10^4 Acm^{-2} at 4.2 K, 0 T have been achieved in the Sn added *ex situ* 1111 IBS wires. [17, 18].

In order to further improve the transport properties of the IBS wires and tapes, it is necessary to investigate the intergranular J_c and the magnetic flux distribution of the material. Magneto-optical imaging (MOI) is an effective technique to visualize the local and real-time distribution of the magnetic flux and reveal the detailed information of the IBS polycrystalline material such as the granularity, homogeneity, intra- and intergranular J_c [14, 19-22]. In this paper, we report a comparative study of the 122 and 1111 IBS tape samples made by our group. One is the $Sr_{1-x}K_xFe_2As_2$ tape with rolling-induced texture made by the low-temperature annealing process with a high transport J_c value of about 10^4 Acm^{-2} at 20 K in self-field, as reported in [23]. The other is the $SmFeAsO_{1-x}F_x$ tape with the highest transport J_c (2.2×10^4 Acm^{-2} at 4.2 K, 0 T) in 1111 IBS wires, which was heat treated at high temperature up to 1100 ^oC for a very short time [18]. Both with transport J_c above 10^4 Acm^{-2} at 4.2 K, 0 T, and the J_c of these two tapes have very different magnetic field dependence. In contrast to the $Sr_{1-x}K_xFe_2As_2$ sample, the J_c of the $SmFeAsO_{1-x}F_x$ sample

This manuscript was published by Superconductor Science & Technology (SuST, IOP) 27, No. 4, 044019, (2014).

decreases very rapidly with increasing field. Therefore, it is interesting to compare their magnetic performance using the MOI technique. By investigating the intergranular J_c at various temperatures and the homogeneity of the local structure, it is suggested that the $Sr_{1-x}K_xFe_2As_2$ sample has a better quality than the $SmFeAsO_{1-x}F_x$ sample, which was caused by a different heat treatment process.

2. Experimental details

The iron-sheathed $Sr_{1-x}K_xFe_2As_2$ tape and $SmFeAsO_{1-x}F_x$ tape were both fabricated by the *ex situ* PIT process. The detail of the starting materials and the cold deformation processes were reported in [23] and [18], respectively. In contrast to the pure $Sr_{1-x}K_xFe_2As_2$ and $SmFeAsO_{1-x}F_x$ tapes, for which no transport J_c was measured, the 5 wt.% Sn added $Sr_{1-x}K_xFe_2As_2$ tapes and 30 wt.% Sn added $SmFeAsO_{1-x}F_x$ tapes showed high transport J_c due to the improved grain connectivity. Therefore, in this work, these two kinds of tapes were selected for a comparative study. As mentioned in the introduction, for the heat treatment, the as-rolled $Sr_{1-x}K_xFe_2As_2$ tapes were sintered at 800-950 ^oC for 5-30 min, while the $SmFeAsO_{1-x}F_x$ tapes were submitted to a short high-temperature annealing at 1100 ^oC for 50 s.

The magneto-optical imaging (MOI) characterization was conducted in the Prof. Tamegai's group at the University of Tokyo. After polishing the superconducting core of the tapes with lapping films, the $Sr_{1-x}K_xFe_2As_2$ and $SmFeAsO_{1-x}F_x$ samples were cut into small rectangular pieces with dimensions of about $0.82\times0.80\times0.10$ mm^3 and $0.96\times0.89\times0.06$ mm^3, respectively. A Bi-substituted iron-garnet indicator film was placed in direct contact with the sample, and the whole assembly was attached to the cold finger of a He-flow cryostat (Microstat-HR, Oxford Instruments). The MO images of the reflected light were obtained by using a cooled CCD camera with 12-bit resolution (ORCA-ER, Hamamatsu). A differential imaging technique was used to enhance the visibility of the local magnetic induction and remove the contrasts induced by the impurity phases and scratches of the garnet film [24, 25]. In the MO images in this paper, as can be seen in figure 2, there are still a few scratches, but they do not affect the analysis of the results. The transport I_c was measured at 4.2 K using short tape samples of 3 cm length with the standard four-probe method and evaluated with a criterion of 1μV/cm. The transport J_c was calculated by dividing the critical current through the cross-sectional area of the superconducting core. The magnetic hysteresis measurements were carried out on a Quantum Design's physical property measurement system (PPMS). The microstructure of samples was analyzed with a Hitachi S4800 scanning electron microscope (SEM)

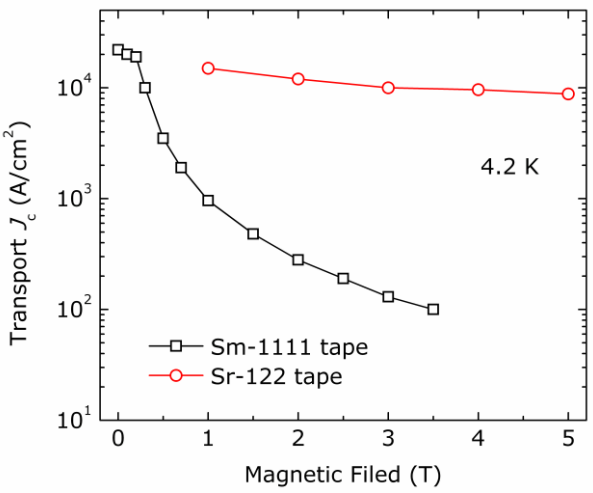

Figure 1. The field dependent transport critical current density J_c of the $Sr_{1-x}K_xFe_2As_2$ (Sr-122) tape and $SmFeAsO_{1-x}F_x$ (Sm-1111) tape at 4.2 K.

3. Results and discussion

Figure 1 shows the field dependent transport J_c of the $Sr_{1-x}K_xFe_2As_2$ tape and $SmFeAsO_{1-x}F_x$ tape at 4.2 K. The magnetic fields were applied parallel to the tape surface. Though the transport J_c of the $SmFeAsO_{1-x}F_x$ tape is as high as 2.2×10^4 Acm^{-2} in self-field, it drops very rapidly with the increase of the applied field. When the applied field is larger than 1 T, the J_c value decreases more than one order of magnitude. One the other hand, for the $Sr_{1-x}K_xFe_2As_2$ tape, the transport J_c decreases very slowly from 1 T to 5 T, suggesting a much better high-field performance. In addition, the value of the transport I_c in self-field for this tape is beyond the maximum (~200 A) of the current source used in the I_c measurement, so its transport J_c in self-field is supposed to be higher than 2.8×10^4 Acm^{-2}.

Figure 2 presents the MO images of the magnetic flux penetration after zero-field cooling (ZFC) the samples to 5 K. The external magnetic fields were applied perpendicular to the sample surface. The bright regions represent the part where the magnetic flux exists. For the $Sr_{1-x}K_xFe_2As_2$ sample, due to the strong shielding currents, the magnetic flux does not penetrate into the sample when the external field is less than 20 mT. When the field is further increased, it gradually moves towards the sample center from the edge, but even when the applied is increased to 50 mT, it still just partially penetrates the sample. This result indicates strong bulk circulating currents in the sample, which can be ascribed to the good grain connectivity and the reduced mismatch of the grains with textured microstructure. The magnetic flux penetration patterns of our tapes are similar to that of the bulk material synthesized by the HIP technique [14], and completely different from that of the weak linked 122 IBS wire sample [21]. For the $SmFeAsO_{1-x}F_x$ sample as shown in figure 2(b), the penetration of the magnetic flux

This manuscript was published by Superconductor Science & Technology (SuST, IOP) 27, No. 4, 044019, (2014).

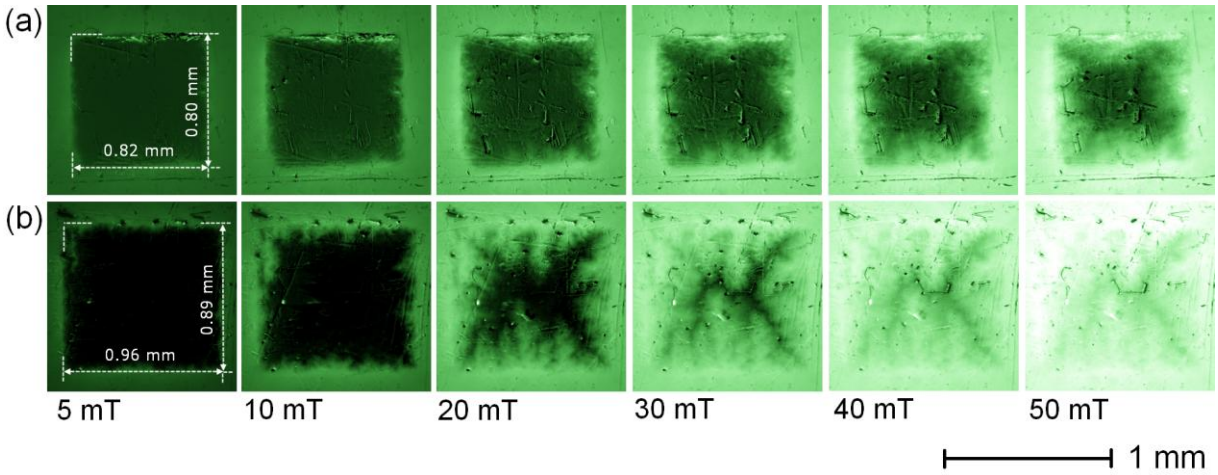

Figure 2. Magneto-optical images of magnetic flux penetration into the (a) $Sr_{1-x}K_xFe_2As_2$ and (b) $SmFeAsO_{1-x}F_x$ rectangular samples in external magnetic fields of 5 mT, 10 mT, 20 mT, 30 mT, 40 mT, and 50 mT after zero-field-cooling (ZFC) the samples to 5 K. The dimensions of the samples are indicated with white dashed lines.

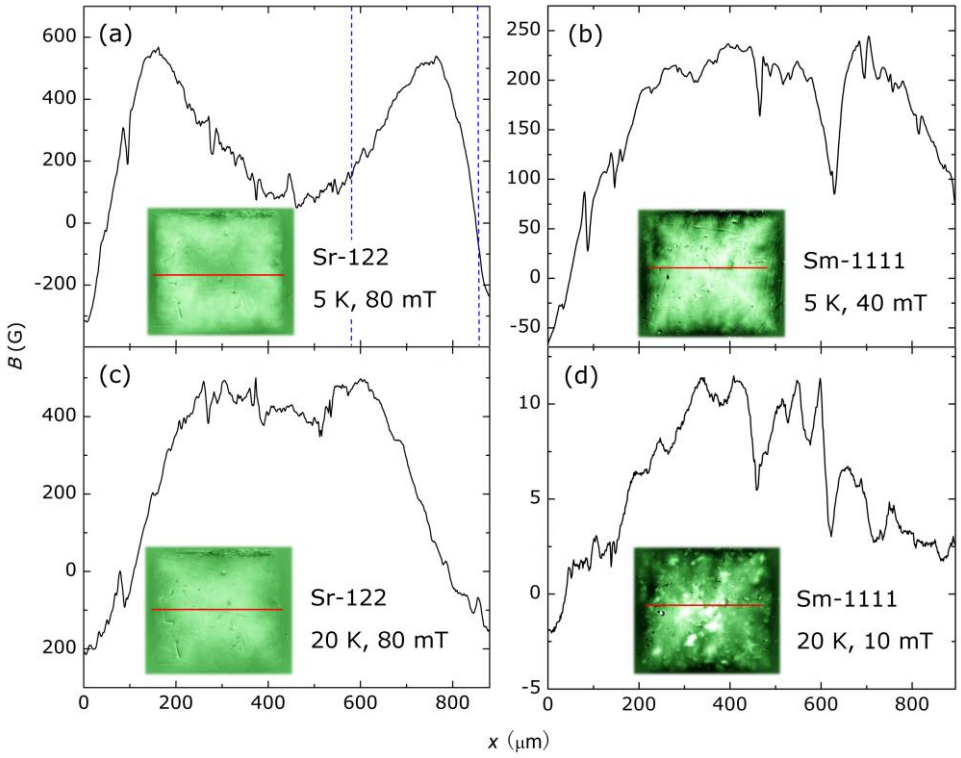

Figure 3. Magneto-optical (MO) images in the remnant state showing trapped magnetic flux and the magnetic induction line profiles along the red lines for the $Sr_{1-x}K_xFe_2As_2$ (Sr-122) and $SmFeAsO_{1-x}F_x$ (Sm-1111) zero-field-cooled (ZFC) samples. (a) Sr-122 sample after cycling the applied field up to 80 mT at 5 K. The blue dashed lines indicate the distance between the sample edge and the front edge of the magnetic flux penetration towards the sample center. (b) Sm-1111 sample after cycling the applied field to 40 mT at 5 K. (c) Sr-122 sample after cycling the applied field to 80 mT at 20 K. (d) Sm-1111 sample after cycling the applied field to 10 mT at 20 K.

into the sample towards the center appears faster than the 122 sample in figure 2(a) with increasing field. However, we can still found the shielding currents go through the whole sample when the field is lower than 20 mT. This result is better than the previously reported Sm-1111 IBS bulk sample [19], indicating the Sn addition in our sample can effectively improve the connectivity between grains. On the other hand, due to the poor crystallinity and large grain-misalignment, the global shielding currents of this sample cannot be kept as well as that of the $Sr_{1-x}K_xFe_2As_2$ sample when increasing the applied fields.

In order to reveal the relationship between the global J_c and the microstructure of the samples, we have investigated the remnant trapped fields after removing the applied fields at 5 K and 20 K for the zero-field-cooled (ZFC) samples. Figure 3(a) shows the magnetic induction line profile along the red line on the MO image. After cycling the field up to 80 mT for 0.2 s at 5 K, the magnetic flux still does not reach the center of the $Sr_{1-x}K_xFe_2As_2$ sample, indicating very strong shielding currents in the sample. In this case, the intergranular J_c can be estimated using the equation [26, 27],

$$J_c = H_{ex}c/4d/\cosh^{-1}[w/(w-2p)] \qquad (1)$$

where H_{ex} is the external field, d is the sample thickness, w is the sample width, and p is the flux penetration distance from the sample edge. In figure 3(a) the right blue dashed line indicates the edge of the sample, and the left blue dashed line indicates the front edge of the flux penetration. Therefore, with H_{ex}=800 Oe, c= 10, d= 100 μm, w= 820 μm and p= 274 μm, the J_c at 5 K for the $Sr_{1-x}K_xFe_2As_2$ sample is calculated to be about 1.1×10^5 Acm^{-2}. In figure 3(c), at 20 K

This manuscript was published by Superconductor Science & Technology (SuST, IOP) 27, No. 4, 044019, (2014).

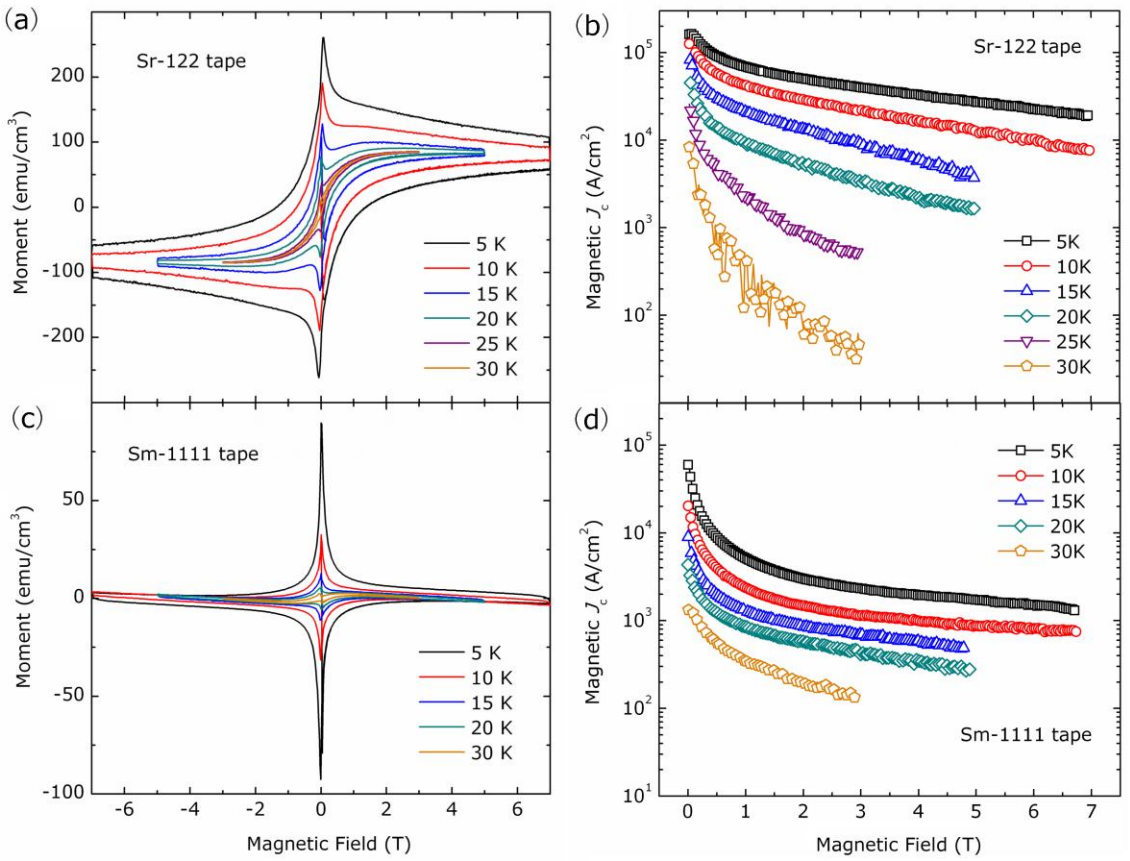

Figure 4. (a) The magnetic hysteresis loops and (b) the field dependent magnetic J_c for the $Sr_{1-x}K_xFe_2As_2$ sample at various temperatures. (c) The magnetic hysteresis loops and (d) the field dependent magnetic J_c for the $SmFeAsO_{1-x}F_x$ sample at various temperatures.

we obtain a very uniform roof top pattern of the fully trapped magnetic flux, and the line profile calculated from the MO image data also shows a roof shape, suggesting bulk currents flow over the whole sample. Since the cycling external field penetrates the whole sample at 20 K, we can estimate the intergranular J_c using the equation,

$$J_c \sim \Delta B/d \qquad (2)$$

where ΔB is the trapped field, and d is the thickness of the sample. According to the magnetic induction line profile, the global J_c at 20 K of this sample is estimated up to 4×10^4 Acm^{-2}. Similarly, as reported in [18], the global J_c at 5 K for the $SmFeAsO_{1-x}F_x$ sample estimated from figure 3(b) is about 3.6×10^4 Acm^{-2}. Though the trapped magnetic flux in the $SmFeAsO_{1-x}F_x$ sample also shows a roof pattern at 5 K, it can be found that the sample is not as homogenous as the 122 sample at 20 K in figure 3(d). We can see some bright local regions in the remnant state MO image, and the curve of the line profile has sharp spikes, indicating that the quality of the grains is not uniform and there are still weak links between grains.

To confirm the intergranular J_c estimated from the MOI results, we measure the magnetic hysteresis at various temperatures of the two samples used in the MO measurements, as shown in figure 4 (a) and (c). The magnetic fields were applied perpendicular to the sample surface. The bulk magnetic J_c can be derived from the magnetic hysteresis loops using the Bean model [28],

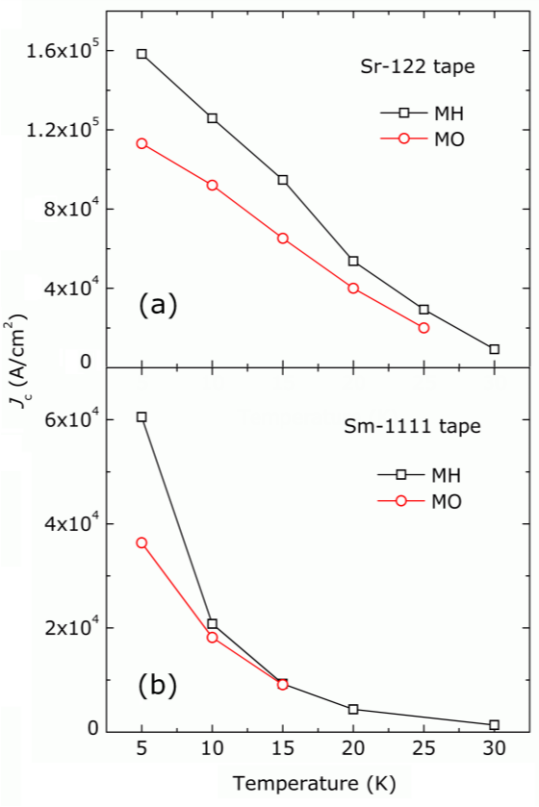

Figure 5. The temperature dependence of the intergranular J_c estimated from the M(H) and MO measurements for the (a) $Sr_{1-x}K_xFe_2As_2$ (Sr-122) and (b) $SmFeAsO_{1-x}F_x$ (Sm-1111) samples.

This manuscript was published by Superconductor Science & Technology (SuST, IOP) 27, No. 4, 044019, (2014).

$$J_c=20\Delta M/[a(1-b/3a)] \quad (3)$$

Where ΔM is the difference between the magnetization when sweeping fields up and down, a and b are the sample widths ($a<b$). The field dependent magnetic J_c of the $Sr_{1-x}K_xFe_2As_2$ and $SmFeAsO_{1-x}F_x$ samples are shown in figure 4(b) and (d), respectively. The temperature dependences of the intergranular J_c of the two samples estimated from the M(H) and MO measurements are plotted in figure 5 (a) and (b). Generally the M(H) measurements are in accordance with the MO measurements. It is found that the magnetic J_c of the $SmFeAsO_{1-x}F_x$ sample decreases quickly with the increase of temperature. Compared with the transport J_c, the values of the magnetic J_c estimated from the M(H) and MO measurement are both larger, indicating there are still inhomogeneity in the superconducting core along the tape length.

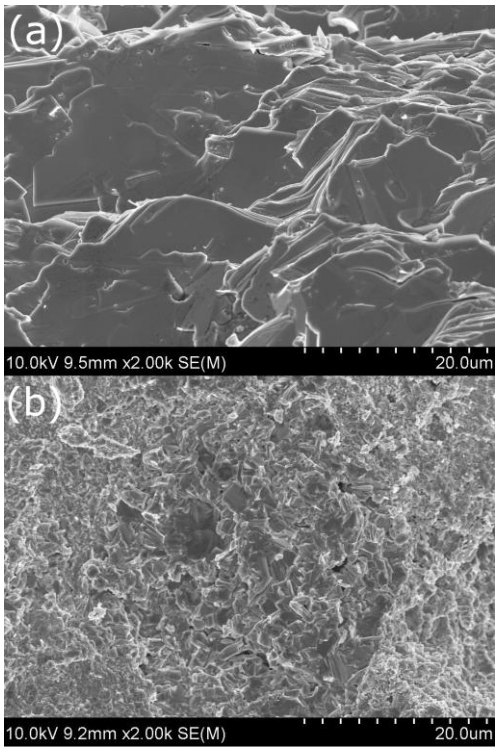

Figure 6. Microstructure of the superconducting cores investigated by SEM. (a) SEM image of the $Sr_{1-x}K_xFe_2As_2$ sample showing a well-coupled planar structure with partial *c*-axis texture. (b) SEM image of the $SmFeAsO_{1-x}F_x$ sample showing an inhomogenous structure with cracks and pores.

By SEM analysis, we examined the microstructure of the samples. In figure 6(a), the superconducting core of the $Sr_{1-x}K_xFe_2As_2$ tape shows a well-coupled planar structure with a flat smooth surface, indicating the *c*-axis texture along the tape surface. There are only a few micro cracks and pores in the grains. For the $SmFeAsO_{1-x}F_x$ sample, as shown in figure 6(b), its grains have a much smaller size than the 122 sample. It is obvious that the quality of the grain is not homogenous, and the grain alignment is not as uniform as the textured $Sr_{1-x}K_xFe_2As_2$ grains, which can result in the weak link at the grain boundaries, and are in consistence with the results of the MOI characterization. The weak performance of the current carrying ability when increasing the fields and temperature of the $SmFeAsO_{1-x}F_x$ tape may be due to the short annealing time and the quick quenching process, which will cause the low quality of grains and the inhomogeneity of microstructures. On the other hand, if increasing the time for the heat treatment, the superconducting core may react with the sheath material, and the loss of fluorine element will be more at the temperature as high as 1100 ^oC. If the heat treatment process for the 1111 IBS tapes can be improved, its transport properties will be largely enhanced in the future.

4. Conclusions

In this work, we use the MOI technique to characterize the superconducting properties of the powder-in-tube $Sr_{1-x}K_xFe_2As_2$ and $SmFeAsO_{1-x}F_x$ tapes. The MO measurement show that the textured $Sr_{1-x}K_xFe_2As_2$ sample heat treated at low temperature has very uniform and well-coupled grains. On the other hand, similar to the $Sr_{1-x}K_xFe_2As_2$ sample, the $SmFeAsO_{1-x}F_x$ tape made by the short high-temperature sintering shows bulk shielding currents in the whole sample region at low temperature around 5 K, but at 20 K the MO measurement reveal inhomogeneity inside the sample, which may cause the rapid decrease of its transport properties when increasing the field and temperature. The results of the MO measurements are in accordance with the M(H) measurements, suggesting that the weak performance of the $SmFeAsO_{1-x}F_x$ tape may be the result of the short annealing time during the heat treatment.

Acknowledgments

This work is partially supported by the National '973' Program (grant No. 2011CBA00105) and the National Natural Science Foundation of China (NSFC) (grant Nos. 51025726, 51172230 and 51202243), and the China–Japan Bilateral Joint Research Project by the JSPS and NSFC.

References

[1] Kamihara Y, Watanabe T, Hirano M and Hosono H 2008 J. Am. Chem. Soc. 130 3296
[2] Ni N, Bud'ko S L, Kreyssig A, Nandi S, Rustan G E, Goldman A I, Gupta S, Corbett J D, Kracher A and Canfield P C 2008 *Phys. Rev.* B 78 014507
[3] Wang X L, Ghorbani S R, Lee S I, Dou S X, Lin C T, Johansen T H, Müller K H, Cheng Z X, Peleckis G, Shabazi M, Qviller A J, Yurchenko V V, Sun G L and Sun D L 2010 Phys. Rev. B 82 024525
[4] Jaroszynski J, Hunte F, Balicas L, Jo Y J, Raičević I, Gurevich A, Larbalestier D C, Balakirev F F, Fang L, Cheng P, Jia Y and Wen H H 2008 Phys. Rev. B 78 174523

This manuscript was published by Superconductor Science & Technology (SuST, IOP) 27, No. 4, 044019, (2014).

[5] Jia Y, Cheng P, Fang L, Luo H Q, Yang H, Ren C, Shan L, Gu C Z and Wen H H 2008 Appl. Phys. Lett.93 032503
[6] Gao Z S, Wang L, Qi Y P, Wang D L, Zhang X P, Ma Y W, Yang H and Wen H H 2008 Supercond. Sci. Technol. 21 112001
[7] Qi Y P, Zhang X P, Gao Z S, Zhang Z Y, Wang L, Wang D L and Ma Y W 2009 Physica C 469 717
[8] Lee S et al 2009 Appl. Phys. Lett. 95 212505
[9] Katase T, Ishimaru Y, Tsukamoto A, Hiramatsu H, Kamiya T, Tanabe K and Hosono H 2011 Nat. Commun. 2 409
[10] Kametani F et al 2009 Appl. Phys. Lett. 95 142502
[11] Wang L, Ma Y W, Wang Q X, Li K, Zhang X X, Qi Y P, Gao Z S, Zhang X P, Wang D L, Yao C and Wang C L 2011 Appl. Phys. Lett. 98 222504
[12] Togano K, Matsumoto A and Kumakura H 2012 Solid State Commun. 152 740
[13] Ma Y W 2012 Supercond. Sci. Technol. 25 113001
[14] Weiss J D, Tarantini C, Jiang J, Kametani F, Polyanskii A A, Larbalestier D C and Hellstrom E E 2012 Nature Mater.11 682
[15] Gao Z S, Ma Y W, Yao C, Zhang X P, Wang C L, Wang D L, Awaji S and Watanabe K 2012 Sci. Rep. 2 998
[16] Togano K, Gao Z S, Matsumoto A and Kumakura H 2013 Supercond. Sci. Technol. 26 115007
[17] Zhang Q J, Wang C L, Yao C, Lin H, Zhang X P, Wang D L, Ma Y W, Awaji S and Watanabe K 2013 J. Appl. Phys 113 123902
[18] Wang C L et al 2013 Supercond. Sci. Technol. 26 075017
[19] Tamegai T, Nakajima Y, Tsuchiya Y, Iyo A, Miyazawa K, Shirage P, Kito H and Eisaki 2009 Physica C 469 915
[20] Prozorov R, Tillman M, Mun E and Canfield P 2009 New J. Phys. 11 035004
[21] Ding Q P, Prombood T, Tsuchiya Y, Nakajima Y and Tamegai T 2012 Supercond. Sci. Technol. 25 035019
[22] Tamegai T, Ding Q P, Inoue H, Taen T, Tsuchiya, Mohan S, Sun Y, Prombood T and Nakajima Y 2013 IEEE Trans. Appl. Supercond. 23 7300304
[23] Ma Y W, Yao C, Zhang X P, Lin H, Wang D L, Matsumoto A, Kumakura H, Tsuhiya Y, Sun Y and Tamegai T 2013 Supercond. Sci. Technol. 26 035011
[24] Soibel A, Zeldov E, Rappaport M, Myasoedov Y, Tamegai T, Ooi S, Konczykowski M and Geshkenbein V 2000 Nature 406 282
[25] Yasugaki M, Itaka K, Tokunaga M, Kameda N and Tamegai T 2002 Phys. Rev. B 65 212502
[26] Nakajima Y, Tsuchiya Y, Taen T, Tamegai T, Okayasu S and Sasase M 2009 Phys. Rev. B 80 012510
[27] Sun Y, Taen T, Tsuchiya Y, Ding Q P, Pyon S, Shi Z X, and Tamegai T 2013 Appl. Phys. Express 6 043101
[28] Bean C P 1964 Rev. Mod. Phys. 36 31